Available online at www.sciencedirect.com

ScienceDirect

Nuclear Physics A 931 (2014) 1066–1071

NUCLEAR PHYSICS A

www.elsevier.com/locate/nuclphysa

Freeze-out radii extracted using two- and three-pion Bose–Einstein correlations in pp, p–Pb, and Pb–Pb collisions at the LHC

Dhevan Raja Gangadharan for the ALICE Collaboration [1]

Lawrence Berkeley National Laboratory, 1 Cyclotron Road, Berkeley, CA 94720, USA

Received 25 August 2014; received in revised form 28 August 2014; accepted 29 August 2014

Available online 2 September 2014

Abstract

We report the results of two- and three-pion Bose–Einstein correlations measured in pp, p–Pb and Pb–Pb collisions with ALICE at the LHC. The femtoscopic radii, which characterize the system size at kinetic freeze-out, are extracted. One- and three-dimensional radii are extracted from two-pion correlations. In addition, one-dimensional radii are extracted also from three-pion correlations. The obtained radii increase with event multiplicity and decrease with pair transverse momentum. At comparable multiplicity, the radii measured in p–Pb collisions are more similar to those in pp collisions than in Pb–Pb collisions. The three-dimensional two-pion radii are compared to hydrodynamic predictions at large event multiplicity.
Published by Elsevier B.V.

Keywords: p–Pb collisions; Femtoscopy; HBT radii

1. Introduction

The study of proton-nucleus collisions is crucial in order to disentangle initial- from final-state effects affecting QCD matter produced in heavy-ion collisions. However, the results obtained from two-particle correlations for p–Pb collisions at $\sqrt{s_{\mathrm{NN}}} = 5.02$ TeV have not been conclusive since they can be explained assuming either a hydrodynamic phase during the evolution of the system or the formation of a Color Glass Condensate (CGC) in the initial state.

[1] A list of members of the ALICE Collaboration and acknowledgments can be found at the end of this issue.

http://dx.doi.org/10.1016/j.nuclphysa.2014.08.098
0375-9474/Published by Elsevier B.V.

The existence of a hydrodynamic phase in high-multiplicity p–Pb collisions is predicted to increase the freeze-out radii by a factor of 1.5–2 with respect to the pp collisions at similar multiplicity [1]. In contrast, a CGC initial state model (IP-GLASMA), without a hydrodynamic phase, predicts similar freeze-out radii in p–Pb and pp collisions [2]. A measurement of the freeze-out radii in the two systems will thus lead to additional experimental constraints on the interpretation of the p–Pb data.

Usually, two-pion Bose–Einstein correlations are used to extract the characteristic radius of the source. However, higher-order Quantum Statistics (QS) correlations can be used as well [3–5]. In particular, higher-order cumulants, from which all lower order correlations are removed, contain a larger QS signal and suppress non-femtoscopic correlations [5].

2. Data analysis

Data from $\sqrt{s} = 7$ TeV pp, $\sqrt{s_{\mathrm{NN}}} = 5.02$ TeV p–Pb, and $\sqrt{s_{\mathrm{NN}}} = 2.76$ Pb–Pb collisions at the LHC recorded with ALICE [6] were analyzed. Approximately 160, 100, and 50 million events were used for pp, p–Pb, and Pb–Pb collisions, respectively.

The Inner Tracking System (ITS) and Time Projection Chamber (TPC) located at mid-rapidity were used for particle tracking. The TPC additionally provides particle identification capabilities through the measurement of the specific ionization energy loss ($\mathrm{d}E/\mathrm{d}x$). The Time Of Flight (TOF) detector was also used to identify particles at higher momenta. To ensure uniform tracking, the z-coordinate of the primary vertex was required to be within ± 10 cm from the detector center.

3. One-dimensional analysis

The one-dimensional analysis was performed in intervals of multiplicity which is defined by the reconstructed number of charged pions. To extract the one-dimensional source radii, we measure two- and three-particle correlation functions as previously performed by ALICE [5,7]. Following [8,9], the two-particle QS distributions, N_2^{QS}, and correlations, C_2^{QS}, are extracted from the measured distributions in intervals of pair transverse momentum $k_{\mathrm{T}} = |p_{\mathrm{T},1} + p_{\mathrm{T},2}|/2$.

The three-particle correlation function

$$C_3(p_1, p_2, p_3) = \alpha_3 \frac{N_3(p_1, p_2, p_3)}{N_1(p_1)N_1(p_2)N_1(p_3)} \tag{1}$$

is defined as the ratio of the inclusive three-particle spectrum over the product of the inclusive single-particle spectra. In analogy to the two-pion case, it is projected onto the Lorentz invariant $Q_3 = \sqrt{q_{12}^2 + q_{31}^2 + q_{23}^2}$ and the average pion transverse momentum $K_{\mathrm{T},3} = \frac{|\vec{p}_{\mathrm{T},1} + \vec{p}_{\mathrm{T},2} + \vec{p}_{\mathrm{T},3}|}{3}$. The numerator of C_3 is formed by taking three particles from the same event. The denominator is formed by taking all three pions from different events. The three-pion Bose–Einstein cumulant is formed subtracting two-pion correlations from Eq. (1) and correcting for final-state-interactions. See Ref. [5] for further details.

Fig. 1 shows the three-pion Gaussian fit parameters. We also show the fit parameters extracted from two-pion correlations in order to compare to those extracted from three-pion cumulants.

For Pb–Pb collisions, the Gaussian radii extracted from three-pion correlations are about 10% smaller than those extracted from two-pion correlations. A clear suppression of both two- and three-pion intercepts below their respective chaotic limits is observed in all multiplicity intervals. The suppression may be caused by non-Gaussian features of the correlation function and also by a finite coherent component of pion emission.

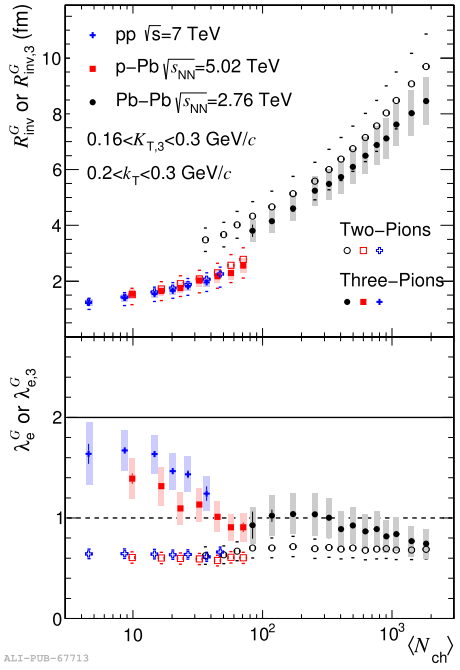

Fig. 1. Two- and three-pion Gaussian fit parameters versus $\langle N_{\rm ch}\rangle$. Top panels show the Gaussian radii $R^{\rm G}_{\rm inv}$ and $R^{\rm G}_{\rm inv,3}$ and bottom panels show the effective Gaussian intercept parameters $\lambda^{\rm G}_{\rm e}$ and $\lambda^{\rm G}_{\rm e,3}$. The dashed and dash-dotted lines represent the chaotic limits for $\lambda^{\rm G}_{\rm e}$ and $\lambda^{\rm G}_{\rm e,3}$, respectively.

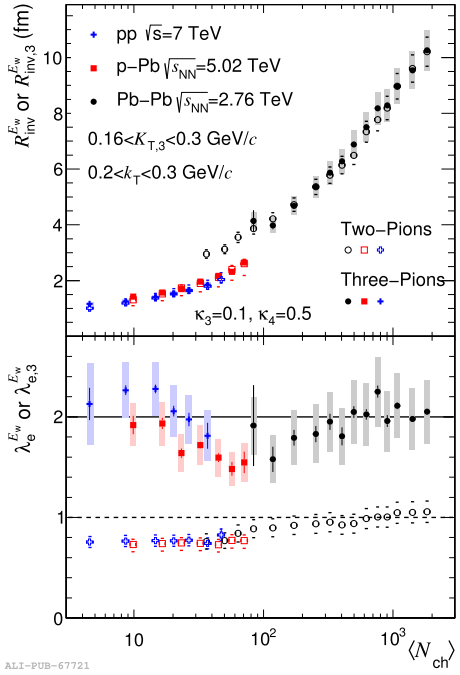

Fig. 2. Two- and three-pion Edgeworth fit parameters versus $\langle N_{\rm ch}\rangle$. Top panels show the Edgeworth radii $R^{E\rm w}_{\rm inv}$ and $R^{E\rm w}_{\rm inv,3}$ and bottom panels show the effective intercept parameters $\lambda^{E\rm w}_{\rm e}$ and $\lambda^{E\rm w}_{\rm e,3}$. The Edgeworth coefficients, κ_3 and κ_4, are fixed to 0.1 and 0.5, respectively. The dashed and dash-dotted lines represent the chaotic limits for $\lambda^{E\rm w}_{\rm e}$ and $\lambda^{E\rm w}_{\rm e,3}$, respectively.

To further address the non-Gaussian features of the correlation functions, we also extract the fit parameters from an Edgeworth expansion of the correlation function as shown in Fig. 2.

4. Three-dimensional analysis

Two-pion correlations were also studied in three dimensions in the *Longitudinal Co-Moving System* frame in which the total longitudinal pair momentum vanishes. The femtoscopic radii are determined independently in three directions: *long* along the beam axis, *out* along the pair transverse momentum, and *side*, perpendicular to the other two. Similar measurements were already performed by ALICE for central Pb–Pb collisions [10] as well as for pp collisions at $\sqrt{s} = 0.9$ and 7 TeV [11,12].

The three-dimensional analysis was performed in four multiplicity classes (0–20%, 20–40%, 40–60% and 60–90%), which are selected by analyzing the signal from the V0 detector. They were defined as fractions of the analyzed event sample sorted by decreasing V0 signal. Seven $k_{\rm T}$ intervals were introduced which were the same for each multiplicity class resulting in 28 independent correlation functions overall.

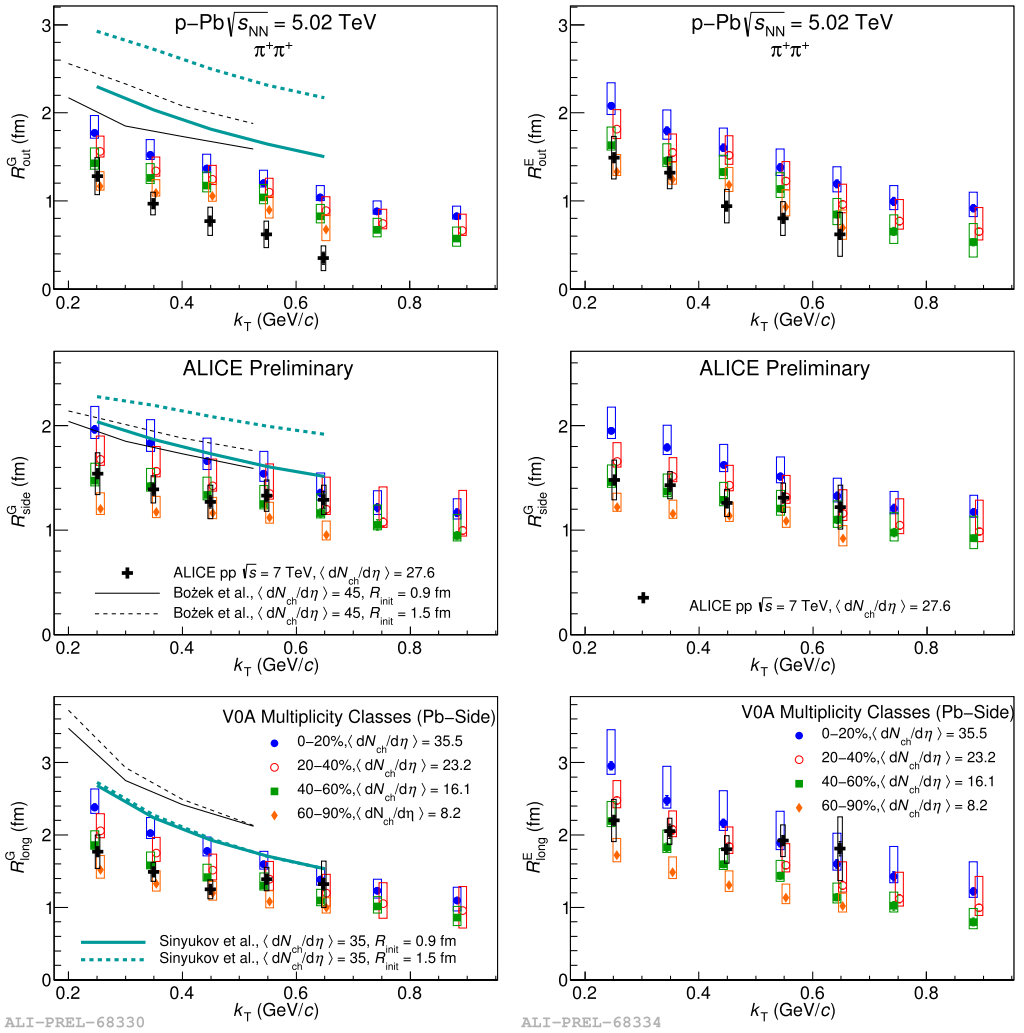

Fig. 3. Femtoscopic radii (left: GGG fit, right: EGE fit) as a function of the pair transverse momentum k_T for four multiplicity classes. Radii from high-multiplicity pp collisions and hydrodynamic model predictions [1,15] are shown as crosses and lines, respectively. The points have been slightly shifted in k_T for visibility.

The obtained correlation functions were found to have a significant non-femtoscopic (mini-jet) contribution. The only models found to describe the structures in a satisfactory way were EPOS 3 [13] and pp PYTHIA 6.4 Perugia-0 which was also used in the ALICE three-dimensional pp analysis [12]. The shapes of the these structures in both models were parametrized and used in the procedure of fitting the data.

The fitting procedure employed the Bowler–Sinyukov approach [8,9] with an additional non-femtoscopic component. Similar to the one-dimensional analysis, we performed Gaussian and non-Gaussian fits to the correlation function. An exponential parametrization in the *out* and *long* directions and a Gaussian parametrization in the *side* direction (EGE) was found to describe the data better than a pure Gaussian parametrization (GGG).

The fitting procedure resulted in 26 sets of femtoscopic radii, for each combination of multiplicity and k_T range (the radius could not be reliably extracted for the two highest k_T ranges in the lowest multiplicity class). They are shown in Fig. 3. The left panel presents the Gaussian radii. The plot also shows ALICE data from pp collisions [12] at the highest multiplicity measured with ALICE, which is slightly higher than the multiplicity measured for the 20–40% range in the p–Pb analysis. The pp radii are lower by 10% for *side* and *long* radii and 20% for *out* radius when compared with p–Pb radii for 20–40% multiplicity class. The differences are bigger in the Gaussian case. The slope of the k_T dependence is also comparable between high multiplicity pp and p–Pb data.

The radii are compared to hydrodynamic model calculations for p–Pb collisions [1,14], which assume the existence of a collectively expanding system. In particular, scenarios with large initial size strongly over predict the radii. The scenarios with lower initial size are closer to the data but are still over predicting the overall magnitude of the radii by 10–30%. Therefore the data challenge the hydrodynamic interpretation of the evolution in p–Pb collisions, however such a scenario cannot be ruled out. Interestingly, the slope of the k_T dependence, which is usually interpreted as a signature of collectivity, is very similar in data and the models in all directions.

The corresponding fit results for the Exponential–Gaussian–Exponential fit are shown in Fig. 3 in the right panel.

5. Conclusions

We reported on the one- and three-dimensional femtoscopic radii extracted from two- and three-pion Bose–Einstein correlations in pp, p–Pb, and Pb–Pb collisions at the LHC with ALICE. While non-femtoscopic backgrounds significantly contribute to two-pion Bose–Einstein correlations, they are suppressed with three-pion cumulant correlations due to the increased QS signal and the removal of two-pion backgrounds.

We found that the radii in p–Pb collisions agree with those pp collisions within 20%, comparable to the sum of systematic uncertainties of both measurements. Non-Gaussian features of the correlation function are found in all three colliding systems.

The high multiplicity data are compared to predictions from two distinct models, each of them based on the mechanism of a fast hydrodynamic expansion of the created medium. The models are found to over predict the R_{out} and R_{long} parameters. However, the introduction of a smaller initial size brings the calculations closer to data. The R_{side} parameter and the slope of the k_T dependence of the radii is reasonably well described.

Models based on the CGC-GLASMA formalism predict sizes similar to those obtained in pp data. Our data is therefore qualitatively consistent with the CGC-GLASMA predictions without a hydrodynamic phase. However, the possibility of a hydrodynamic phase in p–Pb cannot be ruled out based on the measured femtoscopic radii.

References

[1] P. Bozek, W. Broniowski, Phys. Lett. B 720 (2013) 250–253, arXiv:1301.3314.
[2] A. Bzdak, B. Schenke, P. Tribedy, R. Venugopalan, Phys. Rev. C 87 (6) (2013) 064906, arXiv:1304.3403.
[3] N. Neumeister, et al., UA1 Collaboration, Phys. Lett. B 275 (1992) 186–194.
[4] I. Bearden, et al., NA44 Collaboration, Phys. Lett. B 517 (2001) 25–31, arXiv:nucl-ex/0102013.
[5] B.B. Abelev, et al., ALICE Collaboration, arXiv:1404.1194.
[6] K. Aamodt, et al., ALICE Collaboration, J. Instrum. 3 (2008) S08002.
[7] B.B. Abelev, et al., ALICE Collaboration, Phys. Rev. C 89 (2014) 024911, arXiv:1310.7808.

[8] M. Bowler, Phys. Lett. B 270 (1991) 69–74.
[9] Y. Sinyukov, R. Lednicky, S. Akkelin, J. Pluta, B. Erazmus, Phys. Lett. B 432 (1998) 248–257.
[10] K. Aamodt, et al., ALICE Collaboration, Phys. Lett. B 696 (2011) 328–337, arXiv:1012.4035.
[11] K. Aamodt, et al., ALICE Collaboration, Phys. Rev. D 82 (2010) 052001, arXiv:1007.0516.
[12] K. Aamodt, et al., ALICE Collaboration, Phys. Rev. D 84 (2011) 112004, arXiv:1101.3665.
[13] K. Werner, M. Bleicher, B. Guiot, I. Karpenko, T. Pierog, Phys. Rev. Lett. 112 (2014) 232301, arXiv:1307.4379.
[14] V. Shapoval, P. Braun-Munzinger, I.A. Karpenko, Y.M. Sinyukov, arXiv:1304.3815.
[15] Y. Sinyukov, V. Shapoval, private communication.